Modeling of high contrast partially electroded resonators by means of a polynomial approach

P.M. Rabotovao, F.E. Ratolojanahary, Jean-Etienne Lefebvre, A. Raherison, L. Elmaimouni, Tadeusz Gryba, J.G. Yu

Modeling of high contrast partially electroded resonators by means of a polynomial approach

Cite as: J. Appl. Phys. **114**, 124502 (2013); https://doi.org/10.1063/1.4821768
Submitted: 11 March 2013 • Accepted: 03 September 2013 • Published Online: 23 September 2013

P. M. Rabotovao, F. E. Ratolojanahary, J. E. Lefebvre, et al.

Modeling of high contrast partially electroded resonators by means of a polynomial approach

P. M. Rabotovao,[1] F. E. Ratolojanahary,[1] J. E. Lefebvre,[2,a)] A. Raherison,[1] L. Elmaimouni,[3] T. Gryba,[2] and J. G. Yu[4]
[1]*LAPAUF, Université de Fianarantsoa, 301 Fianarantsoa, Madagascar*
[2]*Univ Lille Nord de France, F-59000 Lille, France; UVHC, IEMN-DOAE, 59313 Valenciennes Cedex 9, France; and CNRS, UMR 8520, F-59650 Villeneuve d'Ascq, France*
[3]*ERSITA, Faculté Polydisciplinaire d'Ouarzazate, Université Ibn Zohr, 45000 Ouarzazate, Marocco*
[4]*School of Mechanical and Power Engineering, Henan Polytechnic University, Jiaozuo 454003, People's Republic of China*

(Received 11 March 2013; accepted 3 September 2013; published online 23 September 2013)

This work presents the modeling of high contrast partially electroded resonators by means of a polynomial approach. This method allows easily solving the equations that govern the structure. The boundary, symmetry, and continuity conditions are automatically incorporated into the equations of motion by the use of delta functions for the variables stress (T) and electric displacement (D) and appropriate analytical expression forms for the independent variables, mechanical displacements (u), and electric potential (ϕ). Structure symmetry was used to reduce the number of unknowns. For the zinc oxide (ZnO) resonator in extreme geometrical cases (thin plate and bar cases), a good agreement was obtained between the results of the proposed polynomial approach and those of an analytical approach for both the modal and harmonic analyses. The proposed polynomial approach was used to calculate the 2D resonator electrical admittance (full and partial metallization) near the 1D thickness fundamental mode, and the results highlight the presence of spurious modes. Influence of the metallization rate on the number of spurious modes in the bandwidth is studied. This model can also easily calculate the electromechanical coupling coefficient and the field profiles. Illustrations for both electromechanical coupling coefficient and particle displacement profiles are given for aluminium nitride (AlN), lead zirconate titanate, and ZnO resonators. © *2013 AIP Publishing LLC*. [http://dx.doi.org/10.1063/1.4821768]

I. INTRODUCTION

Since the 1990s, the technology of mobile telecommunications has evolved considerably in the world market. The existence of Micro Electro Mechanical Systems (MEMS), such as piezoelectric resonators, is one factor that accelerates this technology. MEMS is an emerging technology that may fundamentally affect every aspect of our lives.[1] It has the advantages of small size, low-cost, and high-quality factor.[2] Actually, the mobile phones are becoming the most indispensable device for people because of the multiplication of their functionalities (video, TV, Internet, Global Positioning System, etc.). To improve the performance and satisfy the customers in trade, modeling tools are needed.

For modeling the resonators, several models are used in the literature: 1D model is specialized to study analytically one-dimensional structure since it gives access to the main resonance response, and the calculation is simple. However this model does not take into account the effects of structure edges or resonator shape.[3] The Mason model is a model based on equivalent electrical circuits. It is particularly useful and easily used to simulate the electrical behavior of the resonator[4] but is not readily usable to take into account spurious effects. The finite-element method (FEM) is widely used in many different fields with a tremendous ability to solve problems in complex and inhomogeneous media.[5–9] However for large or radiating structures, it can lead to high computational expense and storage requirements which call for specialized calculation techniques giving rise to many alternative improved finite element methods.[10–13] The polynomial method could be an alternative method to treat large or radiating structures as it does not at all require meshing the volume. Large finite and semi-infinite structures could be dealt with using appropriate orthonormal sets of polynomials, Legendre polynomials for large structures, and Laguerre polynomials for semi-infinite structures, for instance. However, until now polynomial method suffers from two major drawbacks: (i) It does not converge satisfactorily in the case of high contrast structures and (ii) it cannot deal with partially electroded structures. In this paper as announced in the perspectives of a previous paper,[14] we propose an extension of the polynomial method in order to obtain satisfactory converged solutions in case of high contrast and partially electroded areas through modeling of finite piezoelectric resonators by Legendre polynomials.

From now on, the former polynomial approach will be named the 1-region polynomial approach and the new one the 3-region polynomial approach. In Sec. II, we define the boundary, symmetry, and continuity conditions according to the geometry of the structure and describe the mathematical formulations giving the physical equations that govern the structure. In Sec. III, we present numerical results. In the first

a)jean-etienne.lefebvre@univ-valenciennes.fr

two paragraphs, through, respectively, a modal and a harmonic analysis, the results obtained for two extreme geometries by the 1-region and the 3-region polynomial approaches are compared with those obtained by an analytical modeling for both a full and a partial metallization. In a third paragraph, the proposed 3-region polynomial approach is exploited to highlight its potentialities. Section IV is a brief conclusion with prospect.

II. MATHEMATICAL FORMULATION

A. Complete structure

The studied structure is a piezoelectric layer sandwiched between two thin ideal metal electrodes (no mass and no stiffness). The piezoelectric layer is partially electroded as shown in Fig. 1. The parameters characterizing the piezoelectric layer are elastic stiffness tensor «c», piezoelectric tensor e, permittivity tensor ε, and mass density ρ. The structure is finite in the x_1 direction and infinite along x_2, and it is assumed that the resonator is polarized by a voltage source V. The coordinate axes x_1, x_2, and x_3 are chosen so that they, respectively, coincide with the crystallographic axes X, Y, and Z with x_3 perpendicular to the constituent layers of the resonator. Throughout this paper, $\exp(i\omega t)$ time dependence is implicit.[5] This structure is divided into three regions: one electroded area (region 1) and two non electroded areas (regions 2 and 3) as shown in Fig. 1. L_1 and W are, respectively, the resonator and electrode widths, and L_3 is the thickness resonator.

We adopt here the following change of variables: $\alpha = W/L_1, q_i = 2x_i/L_i$ (with $i = 1,3$); the normalized variables: $\bar{T}_{ac}^{(R)} = T_{ac}^{(R)}/c_{33}^D$, $\bar{D}_c^{(R)} = D_c^{(R)}/\varepsilon_{33}$; and the normalized physical parameters: $\bar{e}_{cbd} = e_{cbd}/\sqrt{c_{33}^D \varepsilon_{33}}$, $\bar{\varepsilon}_{cd} = \varepsilon_{cd}/\varepsilon_{33}$, and $\bar{c}_{acbd} = c_{acbd}/c_{33}^D$, where $\bar{e}_{cbd}$, $\bar{\varepsilon}_{cd}$, and $\bar{c}_{acbd}$ represent, respectively, the normalized piezoelectric constant, dielectric permittivity, and elastic stiffness. $\bar{T}_{ac}^{(R)}$ and $\bar{D}_c^{(R)}$ are the normalized stress and electric displacement. The bracketed superscript denotes the region number. The subscripts a, b, c, and d take on the values 1 and 3, and summation over repeated subscripts is implied throughout this paper, unless otherwise specified.[15] We also define the normalized elastic viscosity by $\bar{\eta}_{acbd} = \eta_{acbd}.\omega_L/c_{33}^D$, where ω_L is the 1D thickness resonance angular frequency: $\omega_L = \pi/L_3.\sqrt{c_{33}^D/\rho}$ and $c_{33}^D = c_{3333}^E + e_{333}^2/\varepsilon_{33}$. We assume that the crystal of the piezoelectric layer is a hexagonal 6 mm class crystal with a complex normalized elastic stiffness $\bar{c}'_{acbd} = \bar{c}_{acbd} + i\bar{\eta}_{acbd}\Omega$, where Ω is the normalized angular frequency defined by $\Omega = \omega/\omega_L$.[14] The constitutive equations of the structure are defined by

$$\bar{T}_{ac}^S = \sum_R \frac{2}{L_3}\left[(z\delta_{1d} + \delta_{3d})\bar{c}'_{acbd}\frac{\partial u_b^{(R)}}{\partial q_d} + (z\delta_{1d} + \delta_{3d})\frac{\bar{e}_{dac}}{r}\frac{\partial \phi^{(R)}}{\partial q_d}\right]\prod^{(R)}(q_1)\prod(q_3), \quad (1)$$

$$\bar{D}_c^S = \sum_R \frac{2}{L_3}\left[(z\delta_{1d} + \delta_{3d})r\bar{e}_{cdb}\frac{\partial u_b^{(R)}}{\partial q_d} - (z\delta_{1d} + \delta_{3d})\bar{\varepsilon}_{cd}\frac{\partial \phi^{(R)}}{\partial q_d}\right]\prod^{(R)}(q_1)\prod(q_3), \quad (2)$$

where the superscript S denotes the global structure and δ_{ij} is the Kronecker symbol defined as $\delta_{ij} = \begin{cases} 1 \text{ if } i=j \\ 0 \text{ if } i \neq j \end{cases}$, $u_b^{(R)}$ and $\phi^{(R)}$ are, respectively, the components of the mechanical displacement in angstrom and electric potential in volt in the region R, where R is the number of the region in the structure (R = 1, 2, 3), $r = 10^{-10}\sqrt{c_{33}^D/\varepsilon_{33}}$ (V/Å), and $z = L_3/L_1$.

To automatically incorporate the boundary conditions for the variables T and D, we define the rectangular window functions $\Pi(q_3) = \begin{cases} 1 \text{ if } -1 \le q_3 \le 1 \\ 0 \quad \text{otherwise} \end{cases}$, $\Pi^{(1)}(q_1) = \begin{cases} 1 \text{ if } -\alpha \le q_1 \le \alpha \\ 0 \quad \text{otherwise} \end{cases}$, $\Pi^{(2)}(q_1) = \begin{cases} 1 \text{ if } \alpha \le q_1 \le 1 \\ 0 \quad \text{otherwise} \end{cases}$, and $\Pi^{(3)}(q_1) = \begin{cases} 1 \text{ if } -1 \le q_1 \le -\alpha \\ 0 \quad \text{otherwise} \end{cases}$.

The equations of wave propagation in the structure can be written as

$$\frac{2}{L_c}\frac{\partial \bar{T}_{ac}^S}{\partial q_c} = -\rho\omega^2 u_a^S, \quad (3)$$

$$\frac{\partial \bar{D}_c^S}{\partial q_c} = 0, \quad (4)$$

where $u_a^S = \sum_R u_a^{(R)}$, R = 1,2,3.

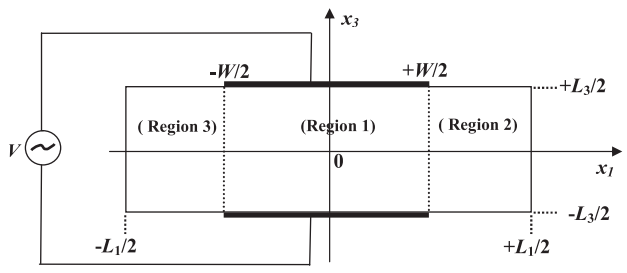

FIG. 1. Schematic view of a partially and symmetrically metalized resonator.

B. Half-structure

Because of the symmetry in the complete structure, it is sufficient to study the half structure with the appropriate boundary, symmetry, and continuity conditions. This allows reducing the number of unknowns which saves both computer storage and time. Thus, the new structure to be studied is divided into two regions, region 1 and region 2 as shown in Fig. 2.

The boundary, symmetry, and continuity conditions in the half structure are given here below.

For the variables T and D, we have

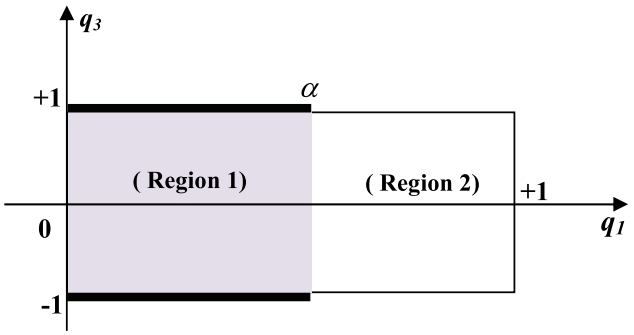

FIG. 2. Half-structure of a partially and symmetrically metalized resonator.

$$\bar{T}_{3c}^{(R)}(q_3 = \pm 1) = 0,$$
$$\bar{T}_{1c}^{(2)}(q_1 = 1) = 0,$$
$$\bar{T}_{13}^{(1)}(q_1 = 0) = 0,$$
$$\bar{T}_{1c}^{(1)}(q_1 = \alpha) = \bar{T}_{1c}^{(2)}(q_1 = \alpha)$$
$$\bar{D}_{1}^{(1)}(q_1 = \alpha) = \bar{D}_{1}^{(2)}(q_1 = \alpha). \tag{5a}$$

For the variables u and D, we have

$$u_1^{(1)}(q_1 = 0) = 0,$$
$$u_a^{(1)}(q_1 = \alpha) = u_a^{(2)}(q_1 = \alpha),$$
$$D_1^{(1)}(q_1 = \alpha) = D_1^{(2)}(q_1 = \alpha),$$
$$D_1^{(1)}(q_1 = 0) = D_1^{(2)}(q_1 = 1) = 0,$$
$$\phi^{(1)}(q_1 = \alpha) = \phi^{(2)}(q_1 = \alpha),$$
$$\phi(q_3 = +1) - \phi(q_3 = -1) = V. \tag{5b}$$

The boundary, symmetry, and continuity conditions are automatically incorporated into the equations of motion using the delta functions for the variables D and T and appropriate analytic forms for the variables u and Φ. In the case of the half structure, Eqs. (1) and (2) can be developed in each region as

$$\bar{T}_{ac}^{(1)} = \frac{2}{L_3}\left[(z\delta_{1d} + \delta_{3d})\bar{c}'_{acbd}\frac{\partial u_b^{(1)}}{\partial q_d} + (z\delta_{1d} + \delta_{3d})\frac{\bar{e}_{dac}}{r}\frac{\partial \phi^{(1)}}{\partial q_d}\right], \tag{6a}$$

$$\bar{T}_{ac}^{(2)} = \frac{2}{L_3}\left[(z\delta_{1d} + \delta_{3d})\bar{c}'_{acbd}\frac{\partial u_b^{(2)}}{\partial q_d} + (z\delta_{1d} + \delta_{3d})\frac{\bar{e}_{dac}}{r}\frac{\partial \phi^{(2)}}{\partial q_d}\right], \tag{6b}$$

$$\bar{D}_{c}^{(1)} = \frac{2}{L_3}\left[(z\delta_{1d} + \delta_{3d})r\bar{e}_{cdb}\frac{\partial u_b^{(1)}}{\partial q_d} - (z\delta_{1d} + \delta_{3d})\bar{\varepsilon}_{cd}\frac{\partial \phi^{(1)}}{\partial q_d}\right], \tag{6c}$$

$$\bar{D}_{c}^{(2)} = \frac{2}{L_3}\left[(z\delta_{1d} + \delta_{3d})r\bar{e}_{cdb}\frac{\partial u_b^{(2)}}{\partial q_d} - (z\delta_{1d} + \delta_{3d})\bar{\varepsilon}_{cd}\frac{\partial \phi^{(2)}}{\partial q_d}\right]. \tag{6d}$$

Substituting Eqs. (6a)–(6d) into Eqs. (3) and (4), with the appropriate boundary, symmetry, and continuity conditions for the variables T and D given by the use of delta functions, yields for the half-structure

$$(z\delta_{1c} + \delta_{3c})\sum_{\mathrm{R}}\frac{\partial \bar{T}_{ac}^{(\mathrm{R})}}{\partial q_c} + \delta_{3c}\sum_{\mathrm{R}}\bar{T}_{ac}^{(\mathrm{R})}[\delta(q_c + 1) - \delta(q_c - 1)]$$
$$- z\delta_{1c}\bar{T}_{ac}^{(2)}\delta(q_c - 1) + z\delta_{1c}(\bar{T}_{ac}^{(2)} - \bar{T}_{ac}^{(1)})\delta(q_c - \alpha)$$
$$+ z\delta_{1c}\delta_{a3}\bar{T}_{ac}^{(1)}\delta(q_c) = -\frac{\rho}{c_{33}^{D}}\frac{L_3}{2}\omega^2\sum_{\mathrm{R}}u_a^{(\mathrm{R})}, \tag{7a}$$

$$(z\delta_{1c} + \delta_{3c})\sum_{\mathrm{R}}\frac{\partial \bar{D}_{c}^{(\mathrm{R})}}{\partial q_c} + \delta_{3c}\bar{D}_{c}^{(2)}[\delta(q_c + 1) - \delta(q_c - 1)]$$
$$+ z\delta_{1c}\bar{D}_{c}^{(1)}\delta(q_c) - z\delta_{1c}\bar{D}_{c}^{(2)}\delta(q_c - 1)$$
$$+ z\delta_{1c}(\bar{D}_{c}^{(2)} - \bar{D}_{c}^{(1)})\delta(q_c - \alpha) = 0 \quad \mathrm{R}=1,2. \tag{7b}$$

The delta functions multiplied by the normal electric displacement component and the normal stress components satisfy the boundary and continuity conditions in the studied structure. Indeed, the terms $\delta_{3c}\bar{T}_{ac}^{(\mathrm{R})}\delta(q_c \pm 1)$, $\delta_{3c}\bar{D}_{c}^{(2)}\delta(q_c \pm 1)$, $\delta_{1c}\bar{T}_{ac}^{(2)}\delta(q_c - 1)$, $\delta_{1c}\ \delta_{a3}\bar{T}_{ac}^{(1)}\delta(q_c)$, $\delta_{1c}\bar{D}_{c}^{(1)}\delta(q_c)$, $\delta_{1c}\bar{D}_{c}^{(2)}\delta(q_c - 1)$, $\delta_{1c}(\bar{T}_{ac}^{(2)} - \bar{T}_{ac}^{(1)})\delta(q_c - \alpha)$ and $\delta_{1c}(\bar{D}_{c}^{(2)} - \bar{D}_{c}^{(1)})\delta(q_c - \alpha)$ in Eqs. (7a) and (7b) impose, respectively, that $\bar{T}_{a3}^{(\mathrm{R})} = 0$ and $\bar{D}_{3}^{(2)} = 0$ for $q_3 = \pm 1$ (boundary condition at the mechanically free surfaces); $\bar{T}_{a1}^{(2)} = 0$ for $q_1 = 1$, $\bar{T}_{31}^{(1)} = 0$ for $q_1 = 0$, $\bar{D}_{3}^{(1)} = 0$ for $q_1 = 0$, and $\bar{D}_{1}^{(2)} = 0$ for $q_1 = 1$ (boundary condition at the lateral surfaces); $\bar{T}_{a1}^{(2)} = \bar{T}_{a1}^{(1)}$ and $\bar{D}_{1}^{(2)} = \bar{D}_{1}^{(1)}$ for $q_1 = \alpha$ (continuity condition). Equations (7a) and (7b) are detailed in Appendix A. The variables $u_b^{(\mathrm{R})}$ and $\phi^{(\mathrm{R})}$ are expanded in a double series of orthonormal functions in $q_1$and q_3 with an analytic form chosen to ensure some of the boundary, symmetry, and continuity conditions.

In region 1:

$$u_1^{(1)}(q_1, q_3) = q_1\sum_{n=0}^{\infty}\sum_{m=0}^{\infty}Q_m^{(1)}(q_1)Q_{2n}(q_3)p_{1,m\,2n}^{(1)}, \tag{8a}$$

$$u_3^{(1)}(q_1, q_3) = \sum_{n=0}^{\infty}\sum_{m=0}^{\infty}Q_m^{(1)}(q_1)Q_{2n+1}(q_3)p_{3,m\,2n+1}^{(1)}, \tag{8b}$$

$$\phi^{(1)}(q_1, q_3) = \frac{V}{2}q_3^3 + (q_3^2 - 1)\sum_{n=0}^{\infty}\sum_{m=0}^{\infty}Q_m^{(1)}(q_1)Q_{2n+1}(q_3)r_{m2n+1}^{(1)}. \tag{8c}$$

In region 2:

$$u_1^{(2)}(q_1, q_3) = u_1^{(1)}(\alpha, q_3) + (q_1 - \alpha) \times \sum_{n=0}^{\infty}\sum_{m=0}^{\infty}Q_m^{(2)}(q_1)Q_{2n}(q_3)p_{1,m\,2n}^{(2)}, \tag{8d}$$

$$u_3^{(2)}(q_1,q_3) = u_3^{(1)}(\alpha,q_3) + (q_1-\alpha) \times \sum_{n=0}^{\infty}\sum_{m=0}^{\infty} Q_m^{(2)}(q_1)Q_{2n+1}(q_3)p_{3,m\,2n+1}^{(2)}, \quad (8e)$$

$$\phi^{(2)}(q_1,q_3) = \phi^{(1)}(\alpha,q_3) + (q_1-\alpha) \times \sum_{n=0}^{\infty}\sum_{m=0}^{\infty} Q_m^{(2)}(q_1)Q_{2n+1}(q_3)r_{m\,2n+1}^{(2)}, \quad (8f)$$

with $Q_j^{(1)}(q_1) = \sqrt{\frac{2j+1}{\alpha}}\mathrm{P}_j\left(\frac{2q_1}{\alpha}-1\right)$, $Q_j^{(2)}(q_1) = \sqrt{\frac{2j+1}{1-\alpha}}\mathrm{P}_j\left(\frac{2q_1}{1-\alpha}-\frac{1+\alpha}{1-\alpha}\right)$, and $Q_k(q_3) = \sqrt{\frac{2k+1}{2}}\mathrm{P}_k(q_3)$, where P_j and P_k are the Legendre polynomial of degree, respectively, j and k. The coefficients $p_{a,m\,n}^{(\mathrm{R})}$ and $r_{m\,n}^{(\mathrm{R})}$ are in angstrom and in volt, respectively. In Eq. (8a), the factor q_1 ensures that $u_1(q_1=0,q_3)=0$. In Eq. (8c), the factor (q_3^2-1) ensures that $\phi^{(1)}(q_1,q_3=1)-\phi^{(1)}(q_1,q_3=-1)=V$. In Eqs. (8d)–(8f), the factor $(q_1-\alpha)$ ensures the continuity of the involved variable at the interface between region 1 and region 2.

Using the symmetry of the structure, we can exploit the odd-even parity for the fields along the q_3 axis, even parity for u_1 and odd parity for u_3 and ϕ. This generates a reduction by one-half of the number of terms in the expansion of the fields with regard to the polynomials $Q(q_3)$. In practice, the summation over the polynomials in Eqs. (8a)–(8f) is truncated at some finite values $m=\mathrm{M}$ and $n=\mathrm{N}$ when higher order terms become essentially negligible.[2] Substituting Eqs. (8a)–(8f) in the constitutive equations (6a)–(6d), themselves substituted into Eqs. (7a) and (7b), multiplying by $Q_j^{(\mathrm{R})}(q_1)$ and $Q_k(q_3)$, and integrating over q_3 from -1 to $+1$ and over q_1 from 0 to α in region 1 and from α to 1 in region 2, we obtain a system of $6\times(\mathrm{M}+1)\times(\mathrm{N}+1)$ linear equations with $6\times(\mathrm{M}+1)\times(\mathrm{N}+1)$ unknowns ($p_{a,m\,n}^{(\mathrm{R})}$ and $r_{m\,n}^{(\mathrm{R})}$) with a parameter Ω

$$(AA + i\Omega.NN).P + BB.R + EE.V = -\Omega^2 MM.P, \quad (9a)$$

$$CC.P + DD.R + FF.V = 0, \quad (9b)$$

with $P = [p_{1,m\,2n}^{(1)}\ p_{3,m\,2n+1}^{(1)}\ p_{1,m\,2n}^{(2)}\ p_{3,m\,2n+1}^{(2)}]^t$ and $R = [r_{m\,2n+1}^{(1)}\quad r_{m\,2n+1}^{(2)}]^t$, where the superscript t denotes a transposed vector or matrix. The matrices *AA*, *MM*, *BB*, *EE*, *CC*, *DD*, *NN*, and *FF* are detailed in Appendix B.

Substituting Eq. (9b) into Eq. (9a) gives a linear equations system

$$[(AA - i\Omega.NN) - BB.DD^{-1}.CC + \Omega^2 MM].P + (EE - BB.DD^{-1}.FF).V = 0. \quad (10)$$

1. Harmonic analysis

Now our goal is to calculate the electrical input admittance Y expressed in normalized form

$$\bar{Y} = Y/i\omega C_o, \quad (11)$$

where $C_o = \varepsilon_{33}S/L_3$ is the static capacitance.

Using the displacement current density defined as $J = i\omega D$, the electric current that flows through the metallic electrode of area S is given by

$$I = i\varepsilon_{33}\omega\int\int_s \bar{D}_3^{(1)}dS. \quad (12)$$

Substituting electric displacement (2) into Eq. (12), we arrive at the following expression for the current I:

$$I = -V + \frac{r}{2}.GG.P, \quad (13)$$

with $GG = \left[\frac{\sqrt{2}}{2}z\bar{e}_{31}GG1\ \ \frac{\sqrt{\alpha}}{\alpha}z\bar{e}_{33}GG3\ \ 0\ \ 0\right]$, where $GG1$ and $GG3$ are given in Appendix A.

Dividing the electric current I in Eq. (13) by the applied voltage V and according to Eq. (11), the normalized electric input admittance is given by

$$\bar{Y} = -1 + \frac{r}{2V}.GG.P. \quad (14)$$

2. Modal analysis

Modal analysis is a specific case of harmonic analysis obtained by cancellation of the electrical excitation. To calculate the resonance frequencies Ω_r, we turn off the voltage source ($V=0$) in Eq. (10), and since the resonance frequencies do not depend on the viscosity tensor, we can simplify the problem by considering a lossless resonator ($\eta=0$ thus $NN=0$).[15] So we obtain

$$MM^{-1}[AA - BB.DD^{-1}.CC].P = -\Omega_r^2 I_d.P, \quad (15)$$

where I_d is the identity matrix. To calculate the antiresonance frequencies Ω_a, we vanish the normalized electric input admittance ($\bar{Y}=0$) in Eq. (14) and we obtain

$$V = \frac{r}{2}.GG.P. \quad (16)$$

Substituting Eq. (16) into Eq. (9) yields an eigen values equation

$$MM^{-1}[AA - BB.DD^{-1}.CC + (EE - BB.DD^{-1}.FF).GG].P = -\Omega_a^2 I_d.P, \quad (17)$$

thus allowing to calculate the antiresonance frequencies Ω_a.

III. NUMERICAL RESULTS

To validate our approach, both the resonance and antiresonance frequencies through a modal analysis and the normalized electric input admittance through a harmonic

TABLE I. Material parameters used in simulations for a ZnO homogeneous resonator.[24]

Parameters	Symbols	ZnO
Mass density (10^3 Kg m^{-3})	ρ	5.676
Elastic stiffness (10^{10} N/m^2)	c	$\begin{bmatrix} 20.97 & 12.11 & 10.51 & 0 & 0 & 0 \\ 12.11 & 20.97 & 10.51 & 0 & 0 & 0 \\ 10.51 & 10.51 & 21.09 & 0 & 0 & 0 \\ 0 & 0 & 0 & 4.25 & 0 & 0 \\ 0 & 0 & 0 & 0 & 4.25 & 0 \\ 0 & 0 & 0 & 0 & 0 & 4.43 \end{bmatrix}$
Elastic viscosity (10^{-3} Pa S)	η	11.96
Piezoelectric constant (C m^{-2})	e	$\begin{bmatrix} 0 & 0 & 0 & 0 & -0.59 & 0 \\ 0 & 0 & 0 & -0.59 & 0 & 0 \\ -0.61 & -0.61 & 1.14 & 0 & 0 & 0 \end{bmatrix}$
Permittivity (10^{-10} F m^{-1})	ε	$\begin{bmatrix} 0.738 & 0 & 0 \\ 0 & 0.738 & 0 \\ 0 & 0 & 0.783 \end{bmatrix}$

analysis are calculated for two extreme geometries (thin plate case $z \ll 1$ and bar case $z \gg 1$) for which an analytical solution is available. Numerical results calculated by the 1-region and 3-region polynomial approaches are compared with results obtained by the analytical modeling. For the polynomial approach with only one region, the electric potential is written as given by Eq. (A20) in Appendix A: the factor $[(q_3^2 - 1) + q_1^2(q_1^2 - \alpha^2)]$ allows imposing the voltage V between the centers of the top and bottom electrodes, on one hand, and between their ends, on the other hand. Moreover, in the calculations two additional terms, $\delta(q_3 - 1)E_1$ and $\delta(q_3 + 1)E_1$, under, respectively, the top and bottom electrodes, are added in the field equations in order to impose in the model the voltage equipotentiality on the electrodes. The material parameters used in simulations are given in Table I.

The associated relative accuracy is calculated as follows for, respectively, the resonance and antiresonance normalized frequencies[14]

$$\varepsilon_{res}(\%) = 100.\frac{|(\Omega_r)_{analytical} - (\Omega_r)_{polynomial}|}{(\Omega_r)_{analytical}} \text{ and}$$

$$\varepsilon_{anti}(\%) = 100.\frac{|(\Omega_a)_{analytical} - (\Omega_a)_{polynomial}|}{(\Omega_a)_{analytical}}.$$

The solutions to be accepted are those for which convergence is obtained as M and N are increased.

TABLE II. Resonance frequencies of a ZnO homogeneous resonator (with $z = 0.01$; $M = N = 9$; $\alpha = 100\%$).

Analytical Ω_r	Polynomial (3-region) Ω_r	ε_{res} (%)	Polynomial (1-region) Ω_r	ε_{res} (%)
0.00831	0.00831	0.00	0.00833	0.28
0.02494	0.02494	0.01	0.02464	1.17
0.04158	0.04156	0.04	0.04097	1.45
0.05821	0.05807	0.22	0.05736	1.46

TABLE III. Antiresonance frequencies of a ZnO homogeneous resonator (with $z = 0.01$; $M = N = 9$; $\alpha = 100\%$).

Analytical Ω_a	Polynomial (3-region) Ω_a	ε_{anti} (%)	Polynomial (1-region) Ω_a	ε_{anti} (%)
0.00865	0.00865	0.03	0.00874	1.08
0.02495	0.02506	0.42	0.02481	0.54
0.04158	0.04163	0.11	0.04105	1.26
0.05821	0.05812	0.15	0.05741	1.37

A. Modal analysis

1. Full metallization ($z \ll 1$ thin plate case and $z \gg 1$ bar case)

The resonance and antiresonance frequencies of a ZnO homogeneous resonator for $z = 0.01$ (thin plate case) and $z = 100$ (bare case) are given, respectively, in Tables II–V with the truncation $M = N = 9$. The results obtained by both polynomial approaches are in very good agreement with the results from the analytical method. These results validate our polynomial approaches for the full metallization resonator case.

2. Partial metallization

Tables VI–IX show the resonance and antiresonance frequencies for a contour mode ZnO resonator with the metallization rates 80% (Tables VI and VIII) and 50% (Tables VIII and IX). The good agreement obtained between 3-region polynomial results and analytical results validates our 3-region polynomial approach for partially electroded resonators. We note that the resonance and antiresonance frequencies increase with the decrease of the length of the electrode which means that the frequency of the resonator can be controlled by the rate of metallization. The discrepancy between the one region polynomial results and analytical results, up to more than 5% in the worst case, can be explained by the contrast at the frontier between the electroded and nonelectroded regions with a difficulty for the series of continuous orthonormal functions expressing the fields to retrieve the exact fields values on each side of the frontier what motivated our new approach.

B. Harmonic analysis

In Figs. 3 and 4 the normalized electric input admittance was calculated for respectively a fully electroded ($\alpha = 100\%$)

TABLE IV. Resonance frequencies of a ZnO homogeneous resonator (with $z = 100$; $M = N = 9$; $\alpha = 100\%$).

Analytical Ω_r	Polynomial (3-region) Ω_r	ε_{res} (%)	Polynomial (1-region) Ω_r	ε_{res} (%)
0.84529	0.84529	0.00	0.84551	0.03
2.68306	2.68287	0.00	2.68369	0.02
4.49031	4.48938	0.02	4.49102	0.02
6.29353	6.29093	0.04	6.29355	0.00

TABLE V. Antiresonance frequencies of a ZnO homogeneous resonator (with z = 100; M = N = 9; α = 100%).

Analytical Ω_a	Polynomial (3-region) Ω_a	ε_{anti} (%)	Polynomial (1-region) Ω_a	ε_{anti} (%)
0.90013	0.90013	0.00	0.90044	0.04
2.70039	2.70018	0.00	2.70108	0.03
4.50065	4.49971	0.02	4.50143	0.02
6.30092	6.29837	0.04	6.30099	0.00

TABLE VI. Resonance frequencies of a ZnO homogeneous resonator (with z = 0.01; M = N = 9; α = 80%).

Analytical Ω_r	Polynomial (3-region) Ω_r	ε_{res} (%)	Polynomial (1-region) Ω_r	ε_{res} (%)
0.00832	0.00832	0.00	0.00830	0.16
0.02506	0.02506	0.03	0.02487	0.74
0.04197	0.04198	0.02	0.04144	1.26
0.05890	0.05889	0.01	0.05800	1.52

TABLE VII. Antiresonance frequencies of a ZnO homogeneous resonator (with z = 0.01; M = N = 9; α = 80%).

Analytical Ω_a	Polynomial (3-region) Ω_a	ε_{anti} (%)	Polynomial (1-region) Ω_a	ε_{anti} (%)
0.00873	0.00873	0.00	0.00863	1.06
0.02622	0.02621	0.01	0.02499	4.68
0.04369	0.04368	0.01	0.04149	5.03
0.06116	0.06112	0.05	0.05803	5.11

TABLE VIII. Resonance frequencies of a ZnO homogeneous resonator (with z = 0.01; M = N = 9; α = 50%).

Analytical Ω_r	Polynomial (3-region) Ω_r	ε_{res} (%)	Polynomial (1-region) Ω_r	ε_{res} (%)
0.00838	0.00838	0.00	0.00828	1.09
0.02570	0.02570	0.00	0.02486	3.24
0.04248	0.04247	0.02	0.04144	2.43
0.05979	0.05976	0.04	0.05803	2.94

TABLE IX. Antiresonance frequencies of a ZnO homogeneous resonator (with z = 0.01; M = N = 9; α = 50%).

Analytical Ω_a	Polynomial (3-region) Ω_a	ε_{anti} (%)	Polynomial (1-region) Ω_a	ε_{anti} (%)
0.00873	0.00873	0.00	0.00893	2.40
0.02580	0.02580	0.00	0.02506	2.84
0.04256	0.04255	0.01	0.04154	2.38
0.05982	0.05979	0.03	0.05809	2.88

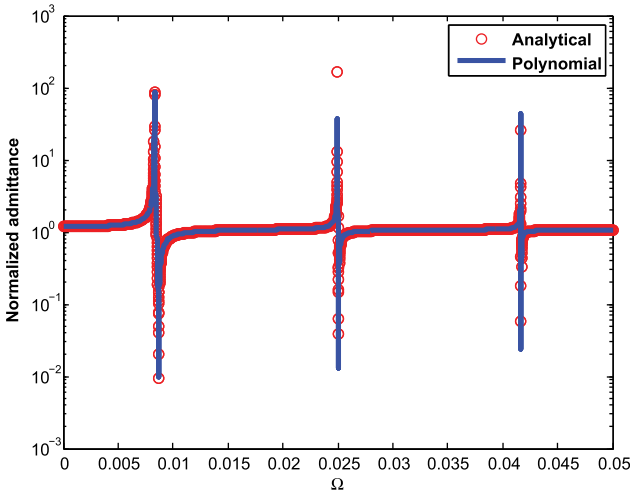

FIG. 3. Normalized admittance of ZnO resonator (z = 0.01; $L_1 = 200\,\mu$m; $L_3 = 2\,\mu$m; M = N = 9; α = 100%) (solid line: 3-region polynomial method; *o* symbol: analytical method).

and a half electroded (α = 50%) ZnO resonator with z = 0.01. Here again, the 3-region polynomial results (solid line) obtained with truncation orders M = N = 9 and analytical results (o symbols) are in good agreement. Moreover, the harmonic analysis retrieves the resonance and antiresonance frequencies obtained by the modal analysis.

C. Model exploitation

To illustrate the capabilities of our 3-region polynomial approach, we have calculated the normalized admittance for two Bulk Acoustic Wave (BAW) resonators laterally bounded (Y 2D) and unbounded (Y 1D) as shown respectively in Figs. 5 and 6. We also calculated the electromechanical coupling coefficient for ZnO, AlN, and PZT resonators as shown in Fig. 7.

Figs. 5(a) and 5(b) show the calculated normalized admittance as a function of the normalized frequency Ωfor,

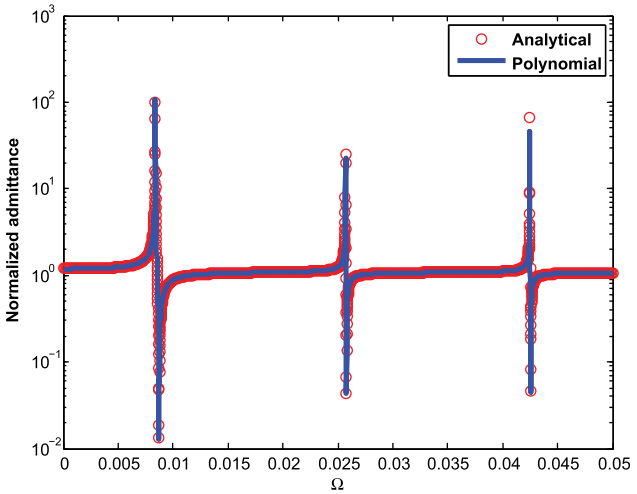

FIG. 4. Normalized admittance of ZnO resonator (z = 0.01; $L_1 = 200\,\mu$m; $L_3 = 2\,\mu$m; M = N = 9; α = 50%) (solid line: 3-region polynomial method; *o* symbol: analytical method).

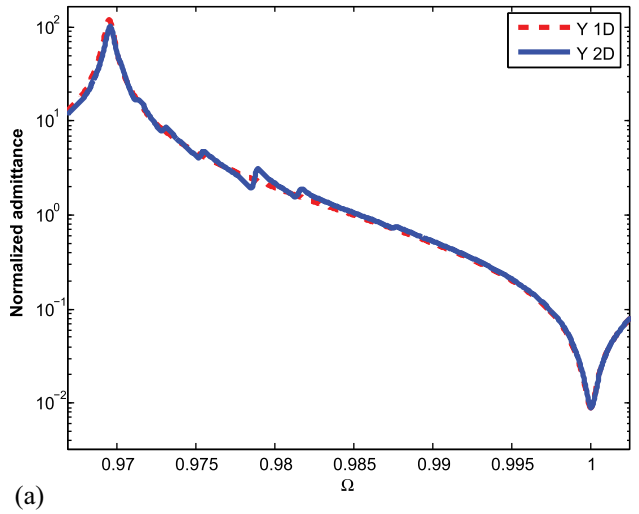

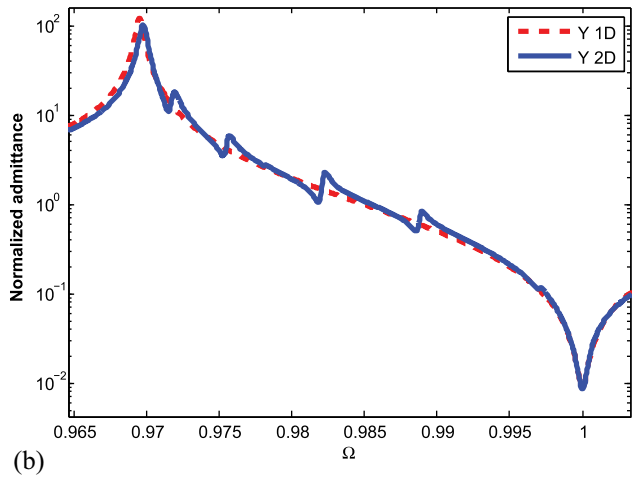

FIG. 5. 1D (dotted line) and 2D (solid line) normalized admittances of a ZnO resonator with (a) full metallization ($\alpha = 100\%$) and (b) partial metallization ($\alpha = 50\%$).

respectively, a fully electroded resonator $\alpha = 100\%$ and a partially electroded one $\alpha = 50\%$. The computing time for the 2000 points and truncation orders $M = N = 9$ are about 20 min for an ordinary computer: CPU 2.80 GHz, Intel Pentium IV, Ram 1 GB. The finite size of the electrode gives rise to spurious resonances contaminating the frequency response close to the fundamental resonance frequency.[16–18] These spurious resonances, not found with the one-dimensional model, cause ripples in the filter bandwidth.[19,20] Fig. 6 shows that the spurious resonances in the frequency bandwidth do no longer exist for a low metallization rate $\alpha = 7\%$.

A characteristic parameter used as a measure of the resonator performance is the electromechanical coupling coefficient.[8] There are several ways for defining the electromechanical coupling coefficient,[21,22] but a definition convenient for experimental work is the effective coupling coefficient expressed as[23] $k_t^2 = \frac{f_p^2 - f_s^2}{f_s^2}$.

Fig. 7 shows the electromechanical coupling coefficient for ZnO, PZT, and AlN resonators for the first mode as a function of the metallization rate α. The PZT resonator shows the largest k_t^2 compared with ZnO and AlN resonators. The maximum k_t^2 is achieved with $\alpha = 75\%$, and this value

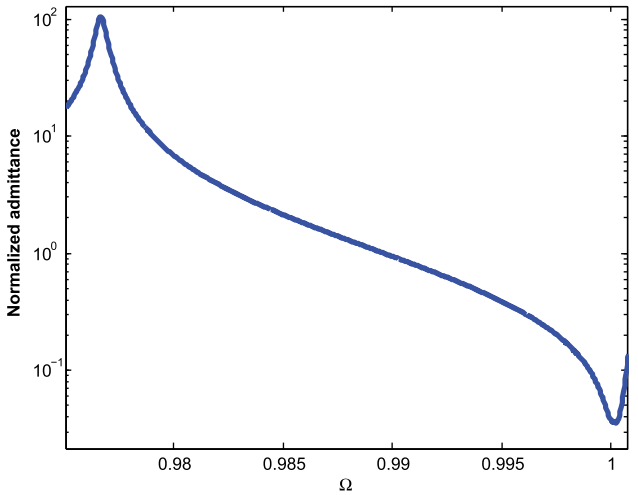

FIG. 6. Normalized admittance of a ZnO partially electroded resonator with $\alpha = 7\%$.

decreases for larger metallization rates. This result highlights the practical advantage to be able to deal with the partially electroded resonator.

Figs. 8(a) and 8(b) show the particle displacement profiles at the normalized resonance frequencies 0.969 and 0.975 for $\alpha = 50\%$. Fig. 8(a) displays the main thickness resonance; Fig. 8(b) displays the main thickness resonance along with a lateral spurious mode.

IV. CONCLUSION

In this paper, we have extended the 1-region polynomial approach to obtain satisfactory converged solutions in case of high contrast and partially electroded areas. Advantage of the resonator symmetry has been taken to reduce the number of unknowns in the field equations. The equations of motion are solved numerically by expanding each mechanical displacement component and the electric potential in a double series of Legendre polynomials. The boundary, symmetry, and continuity conditions are directly incorporated into the

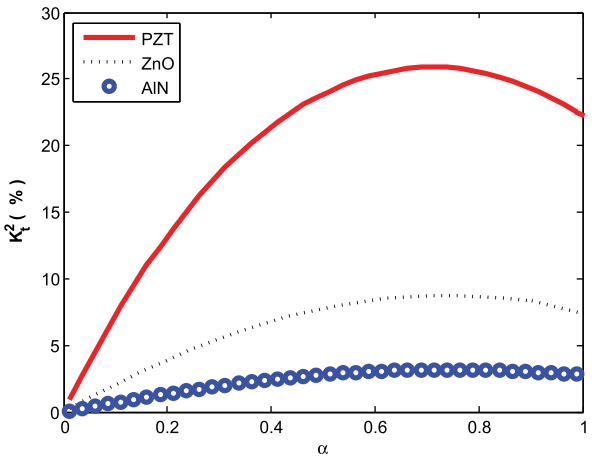

FIG. 7. Electromechanical coupling coefficient for ZnO (dotted line), AlN (o symbol), and PZT (solid line) resonators.

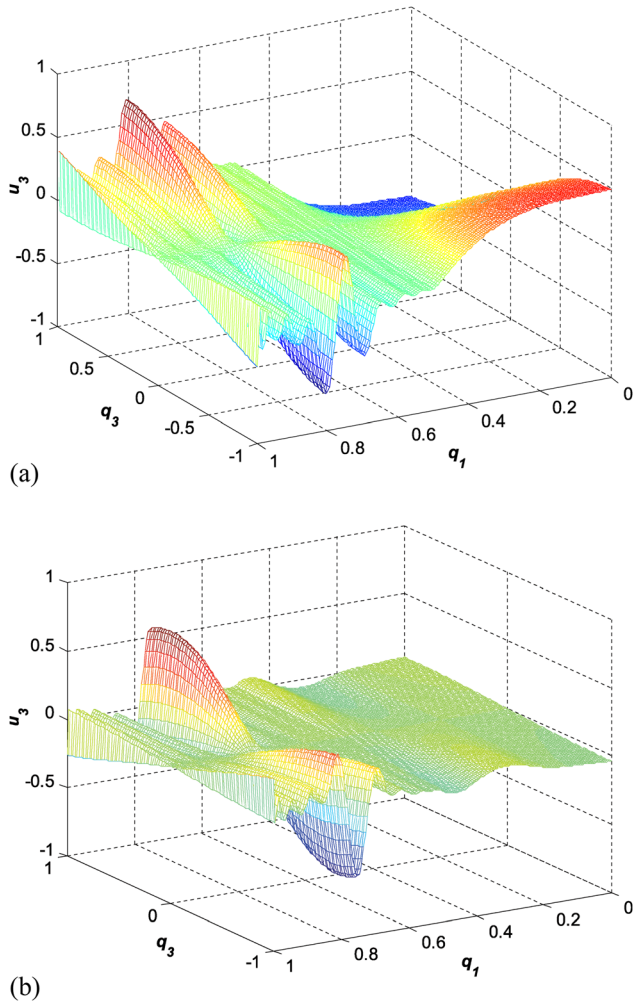

FIG. 8. Particle displacement u_3 profiles into a ZnO partially electroded resonator with $\alpha = 50\%$ (a) for $\Omega_r = 0.969$ and (b) for $\Omega_r = 0.975$.

propagation equation by using delta functions for the variables D and T, and appropriate analytic forms for the variables u and ϕ. Results from both modal and harmonic analyses are presented for the ZnO resonator for extreme geometries. The numerical results for partially and fully electroded resonators are in excellent agreement with the analytical results. To illustrate the application of the 3-region polynomial approach, the coupling coefficient of the ZnO, AlN, and PZT resonators and some particle displacement profiles are calculated. The results highlight the capability of our approach to retrieve the spurious modes in the partially electroded resonators. It is worth noting that, with a single calculation, our method restitutes all types of modes (thickness, lateral, and bar modes) in the structure.

We are now exploring the application of the method to partially electroded resonator with thick electrodes. The technique may also be extended to multi-electrode resonators; however, the details have not yet been worked out.

Finally, we remark that using the appropriate orthonormal sets of functions, we may use the polynomial approach to straightforwardly calculate the acoustic modes in large or semi-infinite structures.

APPENDIX A: PHYSICS EQUATIONS RESOLUTIONS DETAILS

For all calculations in this appendix, to simplify the mathematical writing we use the contracted index notation for all tensors. The constitutive equations (Eq. (6)) are written as:

In region 1:

$$\bar{T}_1^{(1)} = \frac{2}{L_3}\left[z\bar{c}'_{11}\frac{\partial u_1^{(1)}}{\partial q_1} + \bar{c}'_{13}\frac{\partial u_3^{(1)}}{\partial q_3} + \frac{\bar{e}_{31}}{r}\frac{\partial \phi^{(1)}}{\partial q_3}\right], \tag{A1}$$

$$\bar{T}_3^{(1)} = \frac{2}{L_3}\left[z\bar{c}'_{31}\frac{\partial u_1^{(1)}}{\partial q_1} + \bar{c}'_{33}\frac{\partial u_3^{(1)}}{\partial q_3} + \frac{\bar{e}_{33}}{r}\frac{\partial \phi^{(1)}}{\partial q_3}\right], \tag{A2}$$

$$\bar{T}_5^{(1)} = \frac{2}{L_3}\left[z\bar{c}'_{55}\frac{\partial u_3^{(1)}}{\partial q_1} + \bar{c}'_{55}\frac{\partial u_1^{(1)}}{\partial q_3} + z\frac{\bar{e}_{15}}{r}\frac{\partial \phi^{(1)}}{\partial q_1}\right], \tag{A3}$$

$$\bar{D}_1^{(1)} = \frac{2}{L_3}\left[zr\bar{e}_{15}\frac{\partial u_3^{(1)}}{\partial q_1} + r\bar{e}_{15}\frac{\partial u_1^{(1)}}{\partial q_3} - z\bar{\varepsilon}_{11}\frac{\partial \phi^{(1)}}{\partial q_1}\right], \tag{A4}$$

$$\bar{D}_3^{(1)} = \frac{2}{L_3}\left[zr\bar{e}_{31}\frac{\partial u_1^{(1)}}{\partial q_1} + r\bar{e}_{33}\frac{\partial u_3^{(1)}}{\partial q_3} - \bar{\varepsilon}_{33}\frac{\partial \phi^{(1)}}{\partial q_3}\right]. \tag{A5}$$

In region 2:

$$\bar{T}_1^{(2)} = \frac{2}{L_3}\left[z\bar{c}'_{11}\frac{\partial u_1^{(2)}}{\partial q_1} + \bar{c}'_{13}\frac{\partial u_3^{(2)}}{\partial q_3} + \frac{\bar{e}_{31}}{r}\frac{\partial \phi^{(2)}}{\partial q_3}\right], \tag{A6}$$

$$\bar{T}_3^{(2)} = \frac{2}{L_3}\left[z\bar{c}'_{31}\frac{\partial u_1^{(2)}}{\partial q_1} + \bar{c}'_{33}\frac{\partial u_3^{(2)}}{\partial q_3} + \frac{\bar{e}_{33}}{r}\frac{\partial \phi^{(2)}}{\partial q_3}\right], \tag{A7}$$

$$\bar{T}_5^{(2)} = \frac{2}{L_3}\left[z\bar{c}'_{55}\frac{\partial u_3^{(2)}}{\partial q_1} + \bar{c}'_{55}\frac{\partial u_1^{(2)}}{\partial q_3} + z\frac{\bar{e}_{15}}{r}\frac{\partial \phi^{(2)}}{\partial q_1}\right], \tag{A8}$$

$$\bar{D}_1^{(2)} = \frac{2}{L_3}\left[zr\bar{e}_{15}\frac{\partial u_3^{(2)}}{\partial q_1} + r\bar{e}_{15}\frac{\partial u_1^{(2)}}{\partial q_3} - z\bar{\varepsilon}_{11}\frac{\partial \phi^{(2)}}{\partial q_1}\right], \tag{A9}$$

$$\bar{D}_3^{(2)} = \frac{2}{L_3}\left[zr\bar{e}_{31}\frac{\partial u_1^{(2)}}{\partial q_1} + r\bar{e}_{33}\frac{\partial u_3^{(2)}}{\partial q_3} - \bar{\varepsilon}_{33}\frac{\partial \phi^{(2)}}{\partial q_3}\right]. \tag{A10}$$

Substituting the particle displacement and electric potential Eqs. (8a)–(8f) into Eqs. (A1)–(A10) and substituting the stress and electric displacement into Eqs. (7a) and (7b) yields

$$\begin{aligned} &z\frac{\partial \bar{T}_1^{(1)}}{\partial q_1} + \frac{\partial \bar{T}_5^{(1)}}{\partial q_3} + z\frac{\partial \bar{T}_1^{(2)}}{\partial q_1} + \frac{\partial \bar{T}_5^{(2)}}{\partial q_3} - z\bar{T}_1^{(2)}\delta(q_1 - 1) \\ &\quad + \bar{T}_5^{(1)}[\delta(q_3 + 1) - \delta(q_3 - 1)] \\ &\quad + \bar{T}_5^{(2)}[\delta(q_3 + 1) - \delta(q_3 - 1)] + z(\bar{T}_1^{(2)} - \bar{T}_1^{(1)})\delta(q_1 - \alpha) \\ &= -\frac{\rho}{c_{33}^D}\frac{L_3}{2}\omega^2[u_1^{(1)}(q_1, q_3) + u_1^{(2)}(q_1, q_3)], \end{aligned} \tag{A11}$$

$$z\frac{\partial \bar{T}_5^{(1)}}{\partial q_1}+\frac{\partial \bar{T}_3^{(1)}}{\partial q_3}+z\frac{\partial \bar{T}_5^{(2)}}{\partial q_1}+\frac{\partial \bar{T}_3^{(2)}}{\partial q_3}+\bar{T}_3^{(1)}[\delta(q_3+1)-\delta(q_3-1)]+\bar{T}_3^{(2)}[\delta(q_3+1)-\delta(q_3-1)]$$
$$+z\bar{T}_5^{(1)}\delta(q_1)-z\bar{T}_5^{(2)}\delta(q_1-1)+z(\bar{T}_5^{(2)}-\bar{T}_5^{(1)})\delta(q_1-\alpha)=-\frac{\rho}{c_{33}^D}\frac{L_3}{2}\omega^2[u_3^{(1)}(q_1,q_3)+u_3^{(2)}(q_1,q_3)], \tag{A12}$$

$$z\frac{\partial \bar{D}_1^{(1)}}{\partial q_1}+\frac{\partial \bar{D}_3^{(1)}}{\partial q_3}+z\frac{\partial \bar{D}_1^{(2)}}{\partial q_1}+\frac{\partial \bar{D}_3^{(2)}}{\partial q_3}+z\bar{D}_1^{(1)}\delta(q_1)-z\bar{D}_1^{(2)}\delta(q_1-1)+\bar{D}_3^{(2)}[\delta(q_3+1)-\delta(q_3-1)]$$
$$+z(\bar{D}_1^{(2)}-\bar{D}_1^{(1)})\delta(q_1-\alpha)=0. \tag{A13}$$

1. Resolution of Eqs. (A11)-(A13)

By the projection onto the bases $Q_j^{(1)}(q_1)$ and $Q_k(q_3)$, the terms in region 2 are eliminated except the terms of the continuity for $q_1=\alpha$, thus Eqs. (A11)-(A13) give

$$\int_0^{\alpha}\int_{-1}^{1}\left[z\frac{\partial \bar{T}_1^{(1)}}{\partial q_1}+\frac{\partial \bar{T}_5^{(1)}}{\partial q_3}+\bar{T}_5^{(1)}[\delta(q_3+1)-\delta(q_3-1)]+z(\bar{T}_1^{(2)}-\bar{T}_1^{(1)})\delta(q_1-\alpha)=-\frac{\rho}{c_{33}^D}\frac{L_3}{2}\omega^2u_1^{(1)}(q_1,q_3)\right],$$
$$Q_j^{(1)}(q_1)Q_k(q_3)dq_1dq_3 \tag{A14}$$

$$\int_0^{\alpha}\int_{-1}^{1}\left[z\frac{\partial \bar{T}_5^{(1)}}{\partial q_1}+\frac{\partial \bar{T}_3^{(1)}}{\partial q_3}+\bar{T}_3^{(1)}[\delta(q_3+1)-\delta(q_3-1)]+z(\bar{T}_5^{(2)}-\bar{T}_1^{(1)})\delta(q_1-\alpha)+z\bar{T}_5^{(1)}\delta(q_1)=-\frac{\rho}{c_{33}^D}\frac{L_3}{2}\omega^2u_3^{(1)}(q_1,q_3)\right]$$
$$Q_j^{(1)}(q_1)Q_k(q_3)dq_1dq_3, \tag{A15}$$

$$\int_0^{\alpha}\int_{-1}^{1}\left[z\frac{\partial \bar{D}_1^{(1)}}{\partial q_1}+\frac{\partial \bar{D}_3^{(1)}}{\partial q_3}+z\bar{D}_1^{(1)}\delta(q_1)+z(\bar{D}_1^{(2)}-\bar{D}_1^{(1)})\delta(q_1-\alpha)=0\right]Q_j^{(1)}(q_1)Q_k(q_3)dq_1dq_3. \tag{A16}$$

By the projection onto the bases $Q_j^{(2)}(q_1)$ and $Q_k(q_3)$ the terms in region 1 are eliminated except the terms of the continuity for $q_1=\alpha$, thus Eqs. (A11)-(A13) give

$$\int_{\alpha}^{1}\int_{-1}^{1}\left[z\frac{\partial \bar{T}_1^{(2)}}{\partial q_1}+\frac{\partial \bar{T}_5^{(2)}}{\partial q_3}+\bar{T}_5^{(2)}[\delta(q_3+1)-\delta(q_3-1)]+z(\bar{T}_1^{(2)}-\bar{T}_1^{(1)})\delta(q_1-\alpha)-z\bar{T}_1^{(2)}\delta(q_1-1)=-\frac{\rho}{c_{33}^D}\frac{L_3}{2}\omega^2u_1^{(2)}(q_1,q_3)\right]$$
$$Q_j^{(2)}(q_1)Q_k(q_3)dq_1dq_3, \tag{A17}$$

$$\int_{\alpha}^{1}\int_{-1}^{1}\left[z\frac{\partial \bar{T}_5^{(2)}}{\partial q_1}+\frac{\partial \bar{T}_3^{(2)}}{\partial q_3}+\bar{T}_3^{(2)}[\delta(q_3+1)-\delta(q_3-1)]+z(\bar{T}_5^{(2)}-\bar{T}_1^{(1)})\delta(q_1-\alpha)-z\bar{T}_5^{(2)}\delta(q_1)=-\frac{\rho}{c_{33}^D}\frac{L_3}{2}\omega^2u_3^{(2)}(q_1,q_3)\right]$$
$$Q_j^{(2)}(q_1)Q_k(q_3)dq_1dq_3, \tag{A18}$$

$$\int_{\alpha}^{1}\int_{-1}^{1}\left[z\frac{\partial \bar{D}_1^{(2)}}{\partial q_1}+\frac{\partial \bar{D}_3^{(2)}}{\partial q_3}-z\bar{D}_1^{(2)}\delta(q_1-1)+\bar{D}_3^{(2)}[\delta(q_3+1)-\delta(q_3-1)]+z(\bar{D}_1^{(2)}-\bar{D}_1^{(1)})\delta(q_1-\alpha)=0\right]$$
$$Q_j^{(2)}(q_1)Q_k(q_3)dq_1dq_3. \tag{A19}$$

We thus obtain a system of six equations in two unknowns R and P which can be written compactly in a matrix form as

$$(AA+i\Omega.NN).P+BB.R+EE.V=-\Omega^2MM.P$$

for Eqs. (A14), (A15), (A17), and (A18) and

$$CC.P+DD.R+FF.V=0$$

for Eqs. (A16) and (A19).

For the harmonic analysis, the normalized electric input admittance in Eq. (14) is given by

$$\bar{Y} = -1 + \frac{r}{2}\frac{z\bar{e}_{31}\frac{\sqrt{2}}{2}GG1p^{(1)}_{1,m\,2n} + \bar{e}_{33}\frac{\sqrt{\alpha}}{\alpha}GG3p^{(1)}_{3,m\,2n+1}}{V},$$

with $GG1 = Q^{(1)}_m(\alpha)J1^{-1,1,0}_{2n\,0}$ and $GG3 = J1^{0,\alpha,0}_{m\,0}Q_{2n+1}(1)$.
The normalized admittance analytical expression used to validate our model in thin plate case is defined by

$$\bar{Y} = \frac{C^a_o}{C_o}\left[1 + \frac{\tilde{e}^2_{31}}{\tilde{c}_{11}\tilde{\varepsilon}_{33}}.\frac{tg\left(\alpha\frac{\omega L_1}{2V_{cc}}\right)}{\frac{\omega L_1}{2V_{cc}}\left[1 - \sqrt{1 + \frac{\tilde{e}^2_{31}}{\tilde{c}_{11}\tilde{\varepsilon}_{33}}}.tg\left(\alpha\frac{\omega L_1}{2V_{cc}}\right).tg\left[(1-\alpha)\frac{\omega L_1}{2V_{co}}\right]\right]}\right],$$

with $C^a_o = \alpha\tilde{\varepsilon}_{33}z$, $V_{cc} = \sqrt{\frac{\tilde{c}_{11}}{\rho}} = \sqrt{\frac{c_{11}-c_{13}.c_{31}/c_{33}}{\rho}}$, $\tilde{\varepsilon}_{33} = \varepsilon_{33} + \frac{e^2_{33}}{c_{33}}$, and $\tilde{e}_{31} = e_{31} - \frac{e_{33}c_{31}}{c_{33}}$.

The potential expression used in the 1-region polynomial approach is chosen as follows:

$$\phi(q_1, q_3) = \frac{V}{2}q^3_3 + [(q^2_3 - 1) + q^2_1(q^2_1 - \alpha^2)]\sum_{n=0}^{\infty}\sum_{m=0}^{\infty}Q^{(1)}_m(q_1)Q_{2n+1}(q_3)r^{(1)}_{m\,2n+1}. \tag{A20}$$

APPENDIX B: DESCRIPTION OF MATRICES AND INTEGRALS

Here are the matrices of the infinite system of linear equations (8a) and (8b)

$$AA = \begin{bmatrix} AA11\_1 & AA13\_1 & AA11\_12 & AA13\_12 \\ AA31\_1 & AA33\_1 & AA31\_12 & AA33\_12 \\ AA11\_21 & AA13\_21 & AA11\_2 & AA13\_2 \\ AA31\_21 & AA33\_21 & AA31\_2 & AA33\_2 \end{bmatrix}, \quad BB = \begin{bmatrix} BB1\_1 & BB1\_12 \\ BB3\_1 & BB3\_12 \\ BB1\_21 & BB1\_2 \\ BB3\_21 & BB3\_2 \end{bmatrix},$$

$$EE = \begin{bmatrix} EE1\_1 \\ EE3\_1 \\ EE1\_2 \\ EE3\_2 \end{bmatrix}, \quad CC = \begin{bmatrix} CC1\_1 & CC3\_1 & CC1\_12 & CC3\_12 \\ CC1\_21 & CC3\_21 & CC1\_2 & CC3\_2 \end{bmatrix}, \quad DD = \begin{bmatrix} DD1 & DD1\_2 \\ DD2\_1 & DD2 \end{bmatrix},$$

$$NN = \begin{bmatrix} NN11\_1 & NN13\_1 & NN11\_12 & NN13\_12 \\ NN31\_1 & NN33\_1 & NN31\_12 & NN33\_12 \\ NN11\_21 & NN13\_21 & NN11\_2 & NN13\_2 \\ NN31\_21 & NN33\_21 & NN31\_2 & NN33\_2 \end{bmatrix}, \quad FF = \begin{bmatrix} FF\_1 \\ FF\_2 \end{bmatrix}, \quad MM = \begin{bmatrix} MM1^{(1)} & 0 & 0 & 0 \\ 0 & MM1^{(1)} & 0 & 0 \\ MM1^{(2)} & 0 & MM21^{(2)} & 0 \\ 0 & MM3^{(2)} & 0 & MM32^{(2)} \end{bmatrix},$$

with

$$MM1^{(1)} = J1^{0,\alpha,1}_{jm}J1^{-1,1,0}_{kn}, MM1^{(2)} = \alpha\sqrt{1-\alpha}Q^{(1)}_m(\alpha)J1^{\alpha,1,0}_{j0}J1^{-1,1,0}_{kn}, MM21^{(2)} = (J1^{\alpha,1,1}_{jm} - \alpha J1^{\alpha,1,0}_{jm})J1^{-1,1,0}_{kn},$$
$$MM3^{(2)} = \sqrt{1-\alpha}Q^{(1)}_m(\alpha)J1^{\alpha,1,0}_{j0}J1^{-1,1,0}_{kn}, MM32^{(2)} = (J1^{\alpha,1,1}_{jm} - \alpha J1^{\alpha,1,0}_{jm})J1^{-1,1,0}_{kn}.$$

To simplify the calculation we apply the elastic viscosity only for $\bar{c}_{33}$, so the elements of the matrix NN are assumed to be equal to zero except

$$NN33\_1 = \bar{\eta}_{33}J1^{0,\alpha,0}_{jm}J5^{-1,1,0}_{kn},$$

$$NN33\_2 = \bar{\eta}_{33}[J1^{\alpha,1,1}_{jm} - \alpha J1^{\alpha,1,0}_{jm}]J5^{-1,1,0}_{kn}, NN33\_21 = \bar{\eta}_{33}\sqrt{1-\alpha}Q^{(1)}_m(\alpha)J1^{\alpha,1,0}_{j0}J5^{-1,1,0}_{kn},$$

$$AA11\_1 = z^2\bar{c}'_{11}\left[J3^{0,\alpha,1}_{jm} - Q^{(1)}_j(\alpha)\left(Q^{(1)}_m(\alpha) + \alpha\frac{\partial Q^{(1)}_m(\alpha)}{\partial q_1}\right)\right]J1^{-1,1,0}_{kn} + \bar{c}'_{55}J1^{0,\alpha,1}_{jm}J5^{-1,1,0}_{kn},$$

$$AA13\_1 = z[\bar{c}'_{13}J2^{0,\alpha,0}_{jm}J2^{-1,1,0}_{kn} + \bar{c}'_{55}J2^{0,\alpha,0}_{jm}J4^{-1,1,0}_{kn}],$$

$$AA11\_12 = z^2\bar{c}'_{11}Q_j^{(1)}(\alpha)Q_m^{(2)}(\alpha)J1_{kn}^{-1,1,0}, AA13\_12 = 0, AA31\_12 = 0,$$

$$AA31\_1 = z\left[\bar{c}'_{55}(\alpha Q_j^{(1)}(\alpha)Q_m^{(1)}(\alpha) + J4_{jm}^{0,\alpha,1})J2_{kn}^{-1,1,0} + \bar{c}'_{31}J2_{jm}^{0,\alpha,1}J4_{kn}^{-1,1,0}\right],$$

$$AA33\_1 = z^2\bar{c}'_{55}J5_{jm}^{0,\alpha,0}J1_{kn}^{-1,1,0} + \bar{c}'_{33}J1_{jm}^{0,\alpha,0}J5_{kn}^{-1,1,0}, AA33\_12 = z^2\bar{c}'_{55}Q_j^{(1)}(\alpha)Q_m^{(2)}(\alpha)J1_{kn}^{-1,1,0},$$

$$AA11\_21 = -z^2\bar{c}'_{11}Q_j^{(2)}(\alpha)\left(Q_m^{(1)}(\alpha) + \alpha\frac{\partial Q_m^{(1)}(\alpha)}{\partial q_1}\right)J1_{kn}^{-1,1,0} + \alpha\sqrt{1-\alpha}\bar{c}'_{55}Q_m^{(1)}(\alpha)J1_{j0}^{\alpha,1,0}J5_{kn}^{-1,1,0},$$

$$AA13\_21 = -z\bar{c}'_{13}Q_j^{(2)}(1)Q_m^{(1)}(\alpha)J2_{kn}^{-1,1,0},$$

$$AA11\_2 = \bar{c}'_{55}[J1_{jm}^{\alpha,1,1} - \alpha J1_{jm}^{\alpha,1,0}]J5_{kn}^{-1,1,0} + z^2\bar{c}'_{11}[J5_{jm}^{\alpha,1,1} - \alpha J5_{jm}^{\alpha,1,0}]J1_{kn}^{-1,1,0},$$

$$AA13\_2 = z\bar{c}'_{13}[J4_{jm}^{\alpha,1,1} - \alpha J4_{jm}^{\alpha,1,0}]J2_{kn}^{-1,1,0} + z\bar{c}'_{55}[J2_{jm}^{\alpha,1,1} - \alpha J2_{jm}^{\alpha,1,0}]J4_{kn}^{-1,1,0},$$

$$AA31\_21 = -\alpha z\bar{c}'_{55}Q_j^{(2)}(1)Q_m^{(1)}(\alpha)J2_{kn}^{-1,1,0},$$

$$AA33\_21 = -z^2\bar{c}'_{55}Q_j^{(2)}(\alpha)\frac{\partial Q_m^{(1)}(\alpha)}{\partial q_1}J1_{kn}^{-1,1,0} + \bar{c}'_{33}\sqrt{1-\alpha}Q_m^{(1)}(\alpha)J1_{j0}^{\alpha,1,0}J5_{kn}^{-1,1,0},$$

$$AA31\_2 = z\bar{c}'_{55}[J4_{jm}^{\alpha,1,1} - \alpha J4_{jm}^{\alpha,1,0}]J2_{kn}^{-1,1,0} + z\bar{c}'_{31}[J2_{jm}^{\alpha,1,1} - \alpha J2_{jm}^{\alpha,1,0}]J4_{kn}^{-1,1,0},$$

$$AA33\_2 = z^2\bar{c}'_{55}[J5_{jm}^{\alpha,1,1} - \alpha J5_{jm}^{\alpha,1,0}]J1_{kn}^{-1,1,0} + \bar{c}'_{33}[J1_{jm}^{\alpha,1,1} - \alpha J1_{jm}^{\alpha,1,0}]J5_{kn}^{-1,1,0},$$

$$BB1\_1 = (z/r)J2_{jm}^{0,\alpha,0}[\bar{e}_{31}(J2_{kn}^{-1,1,2} - J2_{kn}^{-1,1,0}) + \bar{e}_{15}(J4_{kn}^{-1,1,2} - J4_{kn}^{-1,1,0})], \quad BB1\_12 = 0,$$

$$BB3\_1 = (z^2/r)\bar{e}_{15}J5_{jm}^{0,\alpha,0}[J1_{kn}^{-1,1,2} - J1_{kn}^{-1,1,0}] + (1/r)\bar{e}_{33}J1_{jm}^{0,\alpha,0}[J5_{kn}^{-1,1,2} - J5_{kn}^{-1,1,0}],$$

$$BB3\_12 = (z^2/r)\bar{e}_{15}Q_j^{(1)}(\alpha)Q_m^{(2)}(\alpha)J1_{kn}^{-1,1,0},$$

$$BB1\_21 = -(z/r)\bar{e}_{31}Q_j^{(2)}(1)Q_m^{(1)}(\alpha)[J2_{kn}^{-1,1,2} - J2_{kn}^{-1,1,0}],$$

$$BB1\_2 = (z/r)[\bar{e}_{15}(J2_{jm}^{\alpha,1,1} - \alpha J2_{jm}^{\alpha,1,0})J4_{kn}^{-1,1,0} + \bar{e}_{31}(J4_{jm}^{\alpha,1,1} - \alpha J4_{jm}^{\alpha,1,0})J2_{kn}^{-1,1,0}],$$

$$BB3\_21 = -z^2(\bar{e}_{15}/r)Q_j^{(2)}(\alpha)\frac{\partial Q_m^{(1)}(\alpha)}{\partial q_1}[J1_{kn}^{-1,1,2} - J1_{kn}^{-1,1,0}] + (\bar{e}_{33}/r)\sqrt{1-\alpha}J1_{j0}^{\alpha,1,0}Q_m^{(1)}(\alpha)[J5_{kn}^{-1,1,2} - J5_{kn}^{-1,1,0}],$$

$$BB3\_2 = z^2(\bar{e}_{15}/r)[J5_{jm}^{\alpha,1,1} - \alpha J5_{jm}^{\alpha,1,0}]J1_{kn}^{-1,1,0} + (\bar{e}_{33}/r)[J1_{jm}^{\alpha,1,1} - \alpha J1_{jm}^{\alpha,1,0}]J5_{kn}^{-1,1,0},$$

$$EE1\_1 = 0,\ EE3\_1 = (3\sqrt{2\alpha}/2r)\bar{e}_{33}J1_{j0}^{0,\alpha,0}J4_{k0}^{-1,1,2},$$

$$EE1\_2 = -(3\sqrt{2}z/2r)\bar{e}_{31}Q_j^{(2)}(1)J1_{k0}^{-1,1,2},\ EE3\_2 = (3\sqrt{2(1-\alpha)}/2r)\bar{e}_{33}J1_{j0}^{\alpha,1,0}J4_{k0}^{-1,1,2},$$

$$CC1\_1 = zr[\bar{e}_{15}(J4_{jm}^{0,\alpha,1} + \alpha Q_j^{(1)}(\alpha)Q_m^{(1)}(\alpha)) + \bar{e}_{31}J2_{jm}^{0,\alpha,1}]J2_{kn}^{-1,1,0},$$

$$CC3\_1 = r[z^2\bar{e}_{15}J5_{jm}^{0,\alpha,0}J1_{kn}^{-1,1,0} + \bar{e}_{33}J1_{jm}^{0,\alpha,0}J3_{kn}^{-1,1,0}], CC1\_12 = 0,$$

$$CC3\_12 = z^2r\bar{e}_{15}Q_j^{(1)}(\alpha)Q_m^{(2)}(\alpha)J1_{kn}^{-1,1,0}, CC1\_21 = 0,$$

$$CC1\_21 = -\alpha zr\bar{e}_{15}Q_j^{(2)}(\alpha)Q_m^{(1)}(\alpha)J2_{kn}^{-1,1,0},$$

$$CC3\_21 = -z^2r\bar{e}_{15}Q_j^{(2)}(\alpha)\frac{\partial Q_m^{(1)}(\alpha)}{\partial q_1}J1_{kn}^{-1,1,0} + r\bar{e}_{33}\sqrt{1-\alpha}Q_m^{(1)}(\alpha)J1_{j0}^{\alpha,1,0}J5_{kn}^{-1,1,0},$$

$$CC1\_2 = zr[\bar{e}_{15}(J4_{jm}^{\alpha,1,1} - \alpha J4_{jm}^{\alpha,1,0})J2_{kn}^{-1,1,0} + \bar{e}_{31}(J2_{jm}^{\alpha,1,1} - \alpha J2_{jm}^{\alpha,1,0})J4_{kn}^{-1,1,0}],$$

$$CC3\_2 = r[z^2\bar{e}_{15}(J5_{jm}^{\alpha,1,1} - \alpha J5_{jm}^{\alpha,1,0})J1_{kn}^{-1,1,0} + \bar{e}_{33}(J1_{jm}^{\alpha,1,1} - \alpha J1_{jm}^{\alpha,1,0})J5_{kn}^{-1,1,0}],$$

$$DD\_1 = -z^2\bar{\varepsilon}_{11}J5_{jm}^{0,\alpha,0}[J1_{kn}^{-1,1,2} - J1_{kn}^{-1,1,0}] - \bar{\varepsilon}_{33}J1_{jm}^{0,\alpha,0}[J3_{kn}^{-1,1,2} - J3_{kn}^{-1,1,0}],$$

$$DD1\_2 = -z^2\bar{\varepsilon}_{11}Q_j^{(1)}(\alpha)Q_m^{(2)}(\alpha)J1_{kn}^{-1,1,0},$$

$$DD2\_1 = -\bar{\varepsilon}_{33}\sqrt{1-\alpha}J1_{j0}^{\alpha,1,0}Q_m^{(1)}(\alpha)[J5_{kn}^{-1,1,2} - J5_{kn}^{-1,1,0}] + z^2\bar{\varepsilon}_{11}Q_j^{(2)}(\alpha)\frac{\partial Q_m^{(1)}(\alpha)}{\partial q_1}[J1_{kn}^{-1,1,2} - J1_{kn}^{-1,1,0}],$$

$$DD2 = -[z^2\bar{\varepsilon}_{11}(J5_{jm}^{\alpha,1,1} - \alpha J5_{jm}^{\alpha,1,0})J1_{kn}^{-1,1,0} + \bar{\varepsilon}_{33}(J1_{jm}^{\alpha,1,1} - \alpha J1_{jm}^{\alpha,1,0})J5_{kn}^{-1,1,0}],$$

$$FF\_1 = -\bar{\varepsilon}_{33}3\sqrt{2\alpha}J1_{j0}^{0,\alpha,0}J1_{k0}^{-1,1,1},$$

$$FF\_2 = -\bar{\varepsilon}_{33}3\frac{\sqrt{2(1-\alpha)}}{2}J1_{j0}^{\alpha,1,0}J4_{k0}^{-1,1,2},$$

where

$$J1_{kn}^{-1,1,\gamma} = \int_{-1}^{1} Q_k^*(q_3)q^\gamma Q_n(q_3)dq_3,$$

$$J1_{jm}^{0,\alpha,\gamma} = \int_{0}^{\alpha} Q_j^{*(1)}(q_1)q^\gamma Q_m^{(1)}(q_1)dq_1,$$

$$J1_{jm}^{\alpha,1,\gamma} = \int_{\alpha}^{1} Q_j^{*(2)}(q_1)q^\gamma Q_m^{(2)}(q_1)dq_1,$$

$$J2_{kn}^{-1,1,\gamma} = \int_{-1}^{1} Q_k^*(q_3)\frac{\partial[q^\gamma Q_n(q_3)]}{\partial q_3}dq_3,$$

$$J2_{jm}^{0,\alpha,\gamma} = \int_{0}^{\alpha} Q_j^{*(1)}(q_1)\frac{\partial[q^\gamma Q_m^{(1)}(q_1)]}{\partial q_1}dq_1,$$

$$J2_{jm}^{\alpha,1,\gamma} = \int_{\alpha}^{1} Q_j^{*(2)}(q_1)\frac{\partial[q^\gamma Q_m^{(2)}(q_1)]}{\partial q_1}dq_1,$$

$$J3_{jm}^{0,\alpha,\gamma} = \int_{0}^{\alpha} Q_j^{*(1)}(q_1)\frac{\partial^2[q^\gamma Q_m^{(1)}(q_1)]}{\partial {q_1}^2}dq_1,$$

$$J3_{kn}^{-1,1,\gamma} = \int_{-1}^{1} Q_k^*(q_3)\frac{\partial^2[q^\gamma Q_n(q_3)]}{\partial {q_3}^2}dq_3,$$

$$J4_{kn}^{-1,1,\gamma} = \int_{-1}^{1} Q_k^*(q_3)\frac{\partial[q^\gamma Q_n(q_3)]}{\partial q_3}dq_3,$$

$$J4_{jm}^{0,\alpha,\gamma} = \int_{0}^{\alpha} Q_j^{*(1)}(q_1)\frac{\partial[q^\gamma Q_m^{(1)}(q_1)]}{\partial q_1}dq_1,$$

$$J4_{jm}^{\alpha,1,\gamma} = \int_{\alpha}^{1} Q_j^{*(2)}(q_1)\frac{\partial[q^\gamma Q_m^{(2)}(q_1)]}{\partial q_1}dq_1,$$

$$J5_{kn}^{-1,1,\gamma} = \int_{-1}^{1} Q_k^*(q_3)\frac{\partial}{\partial q_3}\left(\frac{\partial[q^\gamma Q_n(q_3)]}{\partial q_3}\right)dq_3,$$

$$J5_{jm}^{0,\alpha,\gamma} = \int_{0}^{\alpha} Q_j^{*(1)}(q_1)\frac{\partial}{\partial q_1}\left(\frac{\partial[q^\gamma Q_m^{(1)}(q_1)]}{\partial q_1}\right)dq_1,$$

$$J5_{jm}^{\alpha,1,\gamma} = \int_{\alpha}^{1} Q_j^{*(2)}(q_1)\frac{\partial}{\partial q_1}\left(\frac{\partial[q^\gamma Q_m^{(2)}(q_1)]}{\partial q_1}\right)dq_1.$$

[1]P. K. Rao, P. S. S. Babu, A. D. Rani, and D. V. R. K. Reddy, Asian J. Exp. Sci. **22**(3), 351–356 (2008).
[2]L. Elmaimoumi, J. E. Lefebvre, F. E. Ratolojanahary, A. Raherison, B. Bahani, and T. Gryba, Key Eng. Mater. **482**, 11–20 (2011).
[3]N. B. Hassine, Ph.D. dissertation, Université Joseph Fourier (UJF), 2009.
[4]R. Lerch, IEEE Trans. Ultrason. Ferroelect. Freq. Control **37**(2), 233–247 (1990).
[5]L. L. Thompson, Department of Mechanical Engineering, Clemson University, Clemson, South Carolina 29634–0921 (International Engineering Congress and Exposition November 5–10, 2000, Orlando, Florida, USA).
[6]A. Reinhardt, V. Laude, M. Solal, S. Ballandras, and W. Steichen, in *IEEE International Ultrasonics, Ferroelectrics and Frequency Control Joint 50th Anniversary Conference* (2004), pp. 1698–1701.
[7]T. Hayashi, W.-J. Song, and J. L. Rose, Ultrasonics **41**, 175–183 (2003).
[8]T. Makkonen, IEEE Trans. Ultrason. Ferroelectr. Freq. Control **48**(5), 1241–1258 (2001).
[9]T. Alireza *et al.*, in *IEEE Ultrasonics Symposium (IUS)* (IEEE, 2010).
[10]E. Milyutin, Ph.D. dissertation, École Polytechnique Fédérale De Lausanne, 2011.
[11]X. Rui, J. Hu, and Q. H. Liu, Prog. Electromagn. Res. B **21**, 189–201 (2010).
[12]F. Liu and J. Zhao, Int. J. Mech. Sci. **70**, 26–38 (2013).
[13]D.-J. Kim, J. P. Pereira, and C. A. Duarte, Int. J. Numer. Methods Eng. **81**(3), 335–365 (2010).
[14]A. Raherison, J. E. Lefebvre, F. E. Ratolojanahary, L. Elmaimouni, and T. Gryba, J. Appl. Phys. **108**, 104904 (2010).
[15]A. Raherison, F. E. Ratolojanahary, J. E. Lefebvre, and L. Elmaimouni, J. Appl. Phys. **104**(1), 014508 (2008).
[16]K. M. Lakin, G. R. Kline, and K. T. McCarron, IEEE Trans. Microwave Theory Tech. **43**, 2933–2939 (1995).
[17]K. M. Lakin and K. G. Lakin, in *IEEE Ultrasonics Symposium* (2003), pp. 74–79.
[18]H. P. Loebl, C. Metzmacher, R. F. Milsom, R. Mauczok, W. Brand, P. Lok, F. van Straten, and A. Tuinhout, in *IEEE Ultrasonics Symposium* (2003), *pp.* 182–186.
[19]Q. X. Su, P. Kirby, E. Komuro, M. Imura, Q. Zhang, and R. Whatmore, IEEE Trans. Microwave Theory Tech. **49**, 769–778 (2001).
[20]J. Kaitila, M. Ylilammi, J. Ellā, and R. Ainger, in *IEEE Ultrasonics Symposium* (2003), pp. 84–87.
[21]T. Ikeda, *Fundamentals of Piezoelectricity* (Oxford University Press, Oxford, 1996).
[22]S. H. Chang, N. N. Rogacheva, and C. C. Chou, IEEE Ultrason. Ferroelectr. Freq. Control **42**, 630–640 (1995).
[23]ANSI/IEEE Std 176-1987, IEEE Standard on piezoelectricity (The Institute of Electrical and Electronics Engineers, New York, 1987).
[24]J. F. Rosenbaum, *Bulk Acoustic Wave Theory and Devices* (Artech, Boston, 1998).